

Energy dependence study of directed flow in Au+Au collisions using an improved coalescence in AMPT model

Kishora Nayak,¹ Shusu Shi,^{1,*} and Nu Xu^{1,2}

¹*Key Laboratory of Quark & Lepton Physics (MOE) and Institute of Particle Physics, Central China Normal University, Wuhan 430079, China*

²*Institute of Modern Physics, Chinese Academy of Sciences, Lanzhou, China*

(Dated: April 9, 2019)

The rapidity-odd component of directed flow (v_1) of identified hadrons (π^\pm , K^\pm , K_S^0 , p , \bar{p} , ϕ , Ξ^\pm , Λ , $\bar{\Lambda}$) and partons (u , \bar{u} , d , \bar{d} , s , \bar{s}) in Au+Au collisions at various beam energies ($\sqrt{s_{NN}} = 7.7, 11.5, 14.5, 19.6, 27, 39, 54.4, 62.4, 200$ GeV) using a multi-phase transport model are analyzed. A data driven approach (inspired from the experimental analysis) is performed here to distinguish the transported and produced quarks which are found to have different directed flow values at various collision beam energies. The coalescence sum rule (Number of Constituent Quark scaling) violation is observed at lower energies where hadronic matters dominate. The strange quark (s) and ϕ meson slope (dv_1/dy) show a double sign change around 14.5 GeV unlike other partons and hadrons. It suggests that strange quark is more sensitive towards the softening of Equation of State (EoS).

I. INTRODUCTION

The main goal of relativistic heavy-ion collision experiments is to understand the properties and evolution of strong interacting matter, called Quark-Gluon Plasma as well as to explore hadron-quark phase transition. The rapidity-odd component of directed flow, v_1 is an important probe to study the in-medium dynamics as it is sensitive towards the equation of state (EoS) of the produced medium. Directed flow is generated during the nuclear passage time ($2R/\gamma \sim 0.1$ fm/c) and it probes the onset of bulk collective dynamics in the early stage of the collision [1, 2]. As a suggested signature of a first order phase transition, directed flow is sensitive to the existence of the critical point and it plays an important role in the proposed beam energy scan program[3–7]. The first-order harmonic of the Fourier expansion in momentum distribution of emitted particles is characterized as directed flow,

$$v_1 = \langle \cos(\phi - \Psi_{RP}) \rangle \quad (1)$$

where ϕ and Ψ_{RP} are the azimuthal angle and reaction plane angle, respectively [8–10]. The v_1 contains both rapidity-odd and rapidity-even components. Rapidity-odd component ($v_1^{odd}(y) = -v_1^{odd}(-y)$) is referred to the sideward collective motion of emitted hadrons with respect to collision reaction plane. The rapidity-even component even ($v_1^{even}(y) = v_1^{even}(-y)$) is unrelated to the reaction plane and it originates from event-by-event fluctuations in the initial colliding nuclei. In this paper, $v_1(y)$ implicitly refers to the odd component

of directed flow. The transport and hydrodynamic models calculations suggested that the directed flow of baryon v_1 at mid-rapidity ($y \sim 0$) is sensitive to the equation of state of the system [4, 11]. Several hydrodynamic model calculation predict that the negative v_1 -slope near mid-rapidity called as wiggle or anti-flow might be a possible QGP signature [12, 13]. Number-of-constituent-quark (NCQ) scaling is an example of coalescence behavior among quarks. Because of the NCQ scaling, which is observed at RHIC [15, 16] and LHC [17], the higher order flow harmonics like v_2 behaves as if it is developed at the partonic level [19–21]. There are recent experimental measurement of directed flow of various identified hadrons (π^\pm , K^\pm , K_S^0 , p , \bar{p} , ϕ , Λ , $\bar{\Lambda}$) from the STAR collaboration at RHIC over a wide range of colliding beam energies (7.7-200 GeV) [14]. Comprehensive v_1 measurement from STAR [14] supports the coalescence mechanism as the dominant process in particle formation dynamics. There are several studies in heavy-ion collisions to understand the hadron and nuclei formation via coalescence and also hadronization of quarks in heavy-ion collisions [22–26]. In recent articles the importance of coalescence mechanism and energy dependence directed flow are discussed [27–30] and an experimental review of v_1 can be found in Ref [31].

The interplay between NCQ scaling and the transport of initial-state u and d quarks towards mid-rapidity during the collision offers possibilities for new insights [32]. The produced strange (s) and anti-strange (\bar{s}) quark contribute in the resonance (ϕ) formation and hence also plays vital role in understanding the particle formation mechanism. Understanding the strange quarks or particles are very important in order to understand the EoS,

* shiss@mail.ccnu.edu.cn

as the dv_1/dy of ϕ meson also shows a hints of sign change similar to baryon (p , Λ) [14]. An approach to study v_1 performed in this paper is inspired from the STAR experiment at RHIC [14], where a comprehensive measurement of directed flow of identified hadrons are reported in a range of collision energies. The experimental paper verified the coalescence sum rule (NCQ scaling) using v_1 measurement although the NCQ scaling is well known in elliptic flow (v_2) measurement of identified hadrons at RHIC and LHC [15–18]. The model calculation is also compared with the experimental results. The calculation is reasonably well describe the data for mesons over a range of energies. v_1 prediction for Ξ^\pm baryon is also given along with the new energy 54.4 GeV for various hadron species.

The paper is organized in the following sections. Section II provides a brief description about the AMPT event generator [33]. The analysis details of calculating directed flow and the results which include the v_1 of partons and hadrons followed by the slope parameter (dv_1/dy) are discussed in the Sec. III. A summary with final remarks are given in the Sec. IV.

II. THE AMPT MODEL

A multi-phase transport model especially the string-melting version (AMPT-SM) is often used to understand the experimental heavy-ion collision results. The hot and dense matter formed due to relativistic heavy-ion collisions are expected to be in parton degrees of freedom and the AMPT-SM also evolves through the partonic medium, thus makes it a suitable model for interpreting the experimental results. The AMPT-SM version is mainly consist of four parts. The initial conditions are taken from Heavy Ion Jet Inter-action Generator (HIJING) [34]. Scattering among partons are described by Zhangs parton cascade (ZPC) [35] model and for hadronisation it uses the coalescence model. A relativistic transport (ART) model describes the final hadronic evolution [36]. HIJING model includes two body nucleon-nucleon interactions to form excited strings and mini jets via hard and soft processes. The mini-jet parton undergoes scattering before they fragments to parons and subsequently into hadrons. The partonic interaction in ZPC model is described two body partonic elastic cross section as given in Eq. 2.

$$\sigma_{pp} = \frac{9\pi\alpha_S^2}{2\mu^2} \quad (2)$$

In this study the strong coupling constant (α_S) and parton screening mass (μ) are set to be 0.55 and 0.15 fm^{-1} , respectively, leading to $\sigma_{pp} = 1.5 \text{ mb}$.

After partons freeze-out, the hadronization process in AMPT is described by a quark coalescence model. A meson is formed by combining a quark with nearby anti-quark. Similarly, three quarks (anti-quarks) combines to form a baryon (anti-baryon). Here the formation process of mesons or baryons (anti-baryons) are independent of relative momentum among the coalescing partons. Hence, in the the coalescence process, each number of baryons, anti-baryons and mesons in an event are conserved individually. However, in the present study an improved quark coalescence method has been used similarly to the Ref [37]. The constrain which forced separate conservation of the baryons, anti-baryons, and mesons number via the quark coalescence has been removed in the new method. However, the net-baryons and net-strangeness numbers are still conserved for each events. In the new coalescence model, for a meson formation, any available quark searches all available antiquarks and records the closest relative distance (d_M) as the potential coalescence partner. All three closest quarks relative distances are searched and recorded as most potential baryon formation partons and then it searches all other available quarks again to find the smallest average relative distance (d_B) among three quarks to form the baryon. After getting the potential partners for meson and baryon formation, it checks the relative distance for baryon formation. The condition $d_B < d_M * r_{MB}$ has to be satisfied to form a baryon else a meson form. A new coalescence parameter r_{BM} , controls the relative probability of quark to form a baryon rather than meson. The limit of $r_{MB} \rightarrow 0$ and $r_{MB} \rightarrow \infty$ corresponds to almost no anti-baryon (although to keep net-baryon number conservation, a minimum number of baryons would be formed) and meson formation. Similar coalescence procedure is also applied to all anti-quarks.

In this study the new parameter r_{BM} which controls the relative probability to form baryon via coalescence of a quark is set to 0.61. The popcorn parameter PARJ(5) value changed to 0 from the default value 1.0 which controls the relative percentage of the $B\bar{B}$ and $BM\bar{M}$ channels. These r_{MB} parameter value is able to describe the dN/dy of proton yields at mid-rapidity in central Au+Au collisions at $\sqrt{s_{NN}} = 200 \text{ GeV}$ and central Pb+Pb collisions at $\sqrt{s_{NN}} = 2.76 \text{ TeV}$ as given in the Ref [37].

III. ANALYSIS AND RESULTS

In this report, an improved version of AMPT-SM model, $\sigma_{pp} = 1.5 \text{ mb}$ is used to study the directed flow of identified hadrons in mid-central (10-40%)

Au+Au collisions at $\sqrt{s_{NN}} = 7.7, 11.5, 14.5, 19.6, 27, 39, 54.4, 62.4, 200$ GeV, corresponding to RHIC beam energy scan program (BES-I). The centrality is determined using the charged particle multiplicity ($|\eta| < 0.5$). This analysis is inspired from the recent experimental measurement from STAR at RHIC, where a comprehensive v_1 measurement has been performed and coalescence sum rule is verified. The effect of hadronic interaction on directed flow is also studied by changing the hadron cascade time (τ) in the AMPT-SM. The particles reported here are identified from their Pythia-id (PID). The particle selection cuts (e.g. momentum, p , transverse momentum, p_T) are listed in the Tab. III, which is similar to the experimental data [14, 38], in order to have a better comparison.

Hadron	p_T cut (GeV/c)
p, \bar{p}	$0.2 < p_T < 2.0$
π^\pm, K^\pm	$p_T > 0.2, p < 1.6$
$\Lambda, \bar{\Lambda}, K_S^0, \Xi^\pm$	$0.2 < p_T < 5.0$
ϕ	$0.15 < p_T < 10.0$

TABLE I. List of hadrons with their corresponding particle cuts used in this analysis.

The directed flow is calculated by averaging the azimuthal angle (ϕ) using the formula $v_1 = \langle \cos(\phi - \Psi_{RP}) \rangle$ with respect to the reaction plane angle, $\Psi_{RP} = 0$.

Figure 1 shows the directed flow of charged hadrons and ϕ mesons as a function of rapidity for hadron cascade time, $\tau = 0.6$ and 30 fm/c in 10-40% centrality, Au+Au collisions at 7.7, 14.5, 27, 54.4 and 200 GeV. The v_1 of negatively charged hadrons (and positively charged hadrons at higher energies) are found to be not well developed for $\tau = 0.6$ fm/c, because the particles could not get enough time to have hadronic interactions unlike the case of $\tau = 30$ fm/c. However, positively charged hadrons at lower energies for $\tau = 0.6$ fm/c have relatively significant v_1 as compared to higher energies are because of the dominant transported quark at low energies. It is also observed that the hadronic interaction affects v_1 more at higher rapidity. ϕ -meson v_1 for $\tau = 0.6$ and 30 fm/c are found to be similar i.e unaffected by hadronic interaction. This is because of the ϕ meson has small hadronic cross section and longer life time (~ 42 fm/c) than K^{*0} (~ 4.2 fm/c) because of which it decays outside the fireball [39].

Figure 2 shows the directed flow of various identified hadrons (corresponding rows) as function of rapidity in semi-central (10-40%) Au+Au collisions at different collision beam energies (corresponding columns) using AMPT-SM, $\tau = 30$ fm/c. The rapidity dependence of identified hadrons v_1 increases

with decreasing collision beam energy. At highest RHIC energy (200 GeV), particle and anti-particles v_1 values are found to be similar. The v_1 values of baryons and anti-baryons have opposite trend and the difference increases with decrease with energy. The mesons like K^\pm and K_S^0 have similar v_1 values like π^+ and π^- over the measured beam energies. ϕ meson v_1 as a function of rapidity is observed to be similar to baryons (p, Λ, Ξ^-), which have a strong positive slope at lower energy unlike the mesons (K^\pm, K_S^0, π^\pm).

Figure 3 shows the comparison of directed flow as a function of rapidity between experimental data from STAR at RHIC [14] and AMPT-SM ($\sigma_{pp} = 1.5$ mb, $\tau = 30$ fm/c) calculation for different identified hadrons at various collision energies. The AMPT-SM is relatively well describe the experimental data for mesons than baryons and anti-baryons over the calculated energy ranges.

The strength of directed flow signal at mid-rapidity is usually characterized by the linear term, F , in the equation $v_1(y) = Fy + F_3y^3$ [14] or by the slope (F') parameter of the fit function $v_1(y) = F'y + C$ [38]. Here, the slope parameter F' is denoted as dv_1/dy . By using the cubic fit function one can reduce sensitivity to the rapidity range in which the fitting is performed. However, in order to have a better comparison we have used the linear fit function similar to the experimental STAR result [14]. The fitting range for various hadron species are $|y| < 0.8$ for all measured particles except for ϕ meson which is fitted in the rapidity range, $|y| < 0.6$.

The collision beam energy dependence of directed flow slope, dv_1/dy , for baryons ($p, \bar{p}, \Lambda, \bar{\Lambda}, \Xi^-, \Xi^+$) and mesons ($\pi^-, \pi^+, K^+, K^-, K_S^0, \phi$) are shown in Fig. 4 (a) and Fig. 4 (b), respectively. The dv_1/dy of measured baryons such as p, Λ , and Ξ^- are found to have similar value like their anti-particles $\bar{p}, \bar{\Lambda}$, and Ξ^+ which have also similar slope within the uncertainty over the measured energy ranges. All the measured baryons have positive dv_1/dy where as their anti-particles have negative slope values. In AMPT-SM, the sign change of baryons' (p and Λ) slope is not observed unlike observed in STAR experiment [14]. The dv_1/dy of π^- and π^+ are similar; K^+ and K^- values are also similar except for lower energies (< 19.6 GeV) and their average value corresponds to slope of K_S^0 meson. All the mesons and their anti-particles except ϕ resonance have negative dv_1/dy below 39 GeV collision energy unlike the corresponding STAR results [14]. Overall magnitude of baryons and anti-baryons dv_1/dy are larger than the mesons and their anti-particles.

Figure 5 shows the ϕ meson slope calculated by using different fitting ranges for both linear and

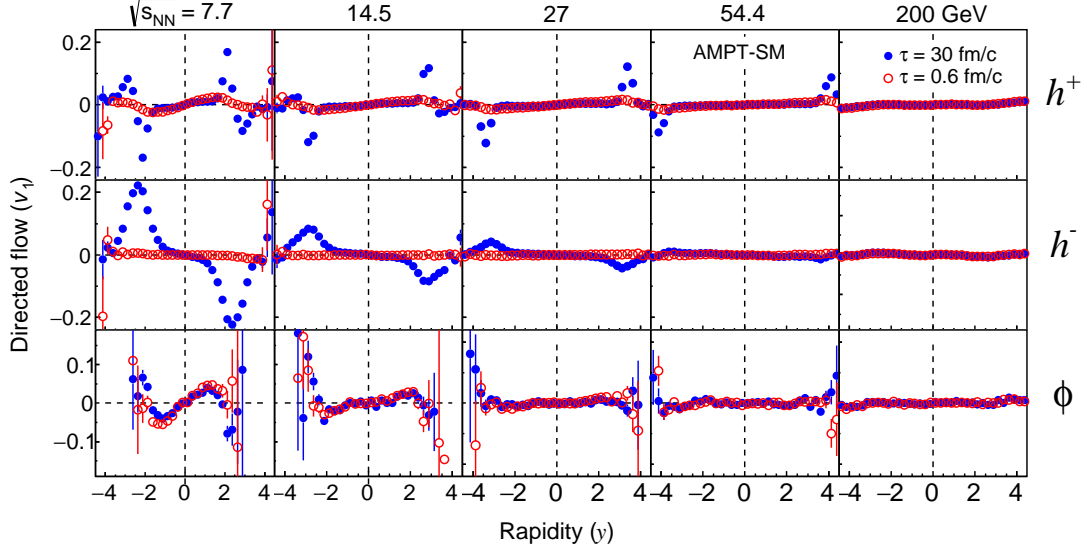


FIG. 1. Directed flow (v_1) as a function of rapidity (y) for hadron cascade time, $\tau = 30$ fm/c (solid marker), 0.6 fm/c (open marker). Upper, middle and lower rows correspond to positively, negatively charged hadrons and ϕ meson, respectively in 10-40% centrality, Au+Au collisions at $\sqrt{s_{NN}} = 7.7, 14.5, 27, 54.4$ and 200 GeV using AMPT-SM.

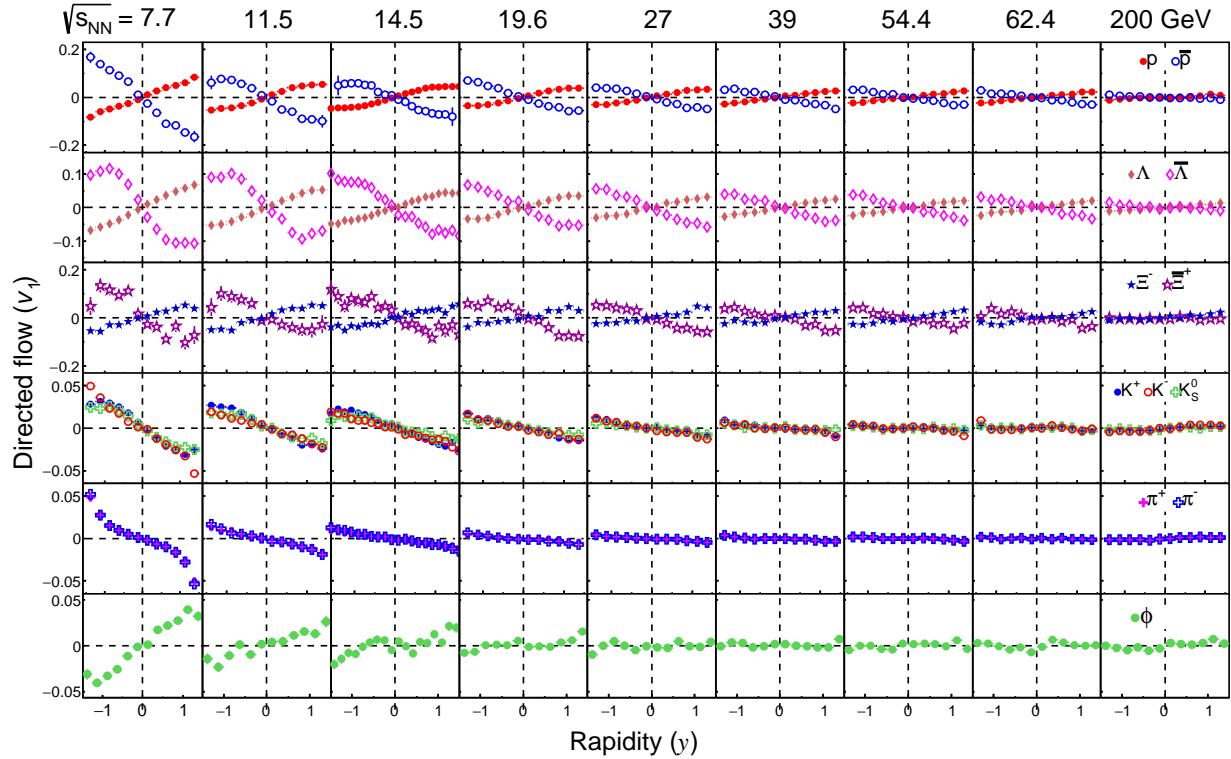


FIG. 2. (Color online) Directed flow (v_1) as a function of rapidity (y) for hadron cascade time, $\tau = 30$ fm/c for different identified hadrons (rows) in Au+Au collisions at $\sqrt{s_{NN}} = 7.7, 11.5, 14.5, 19.6, 27, 39, 54.4, 62.4$ and 200 GeV (columns).

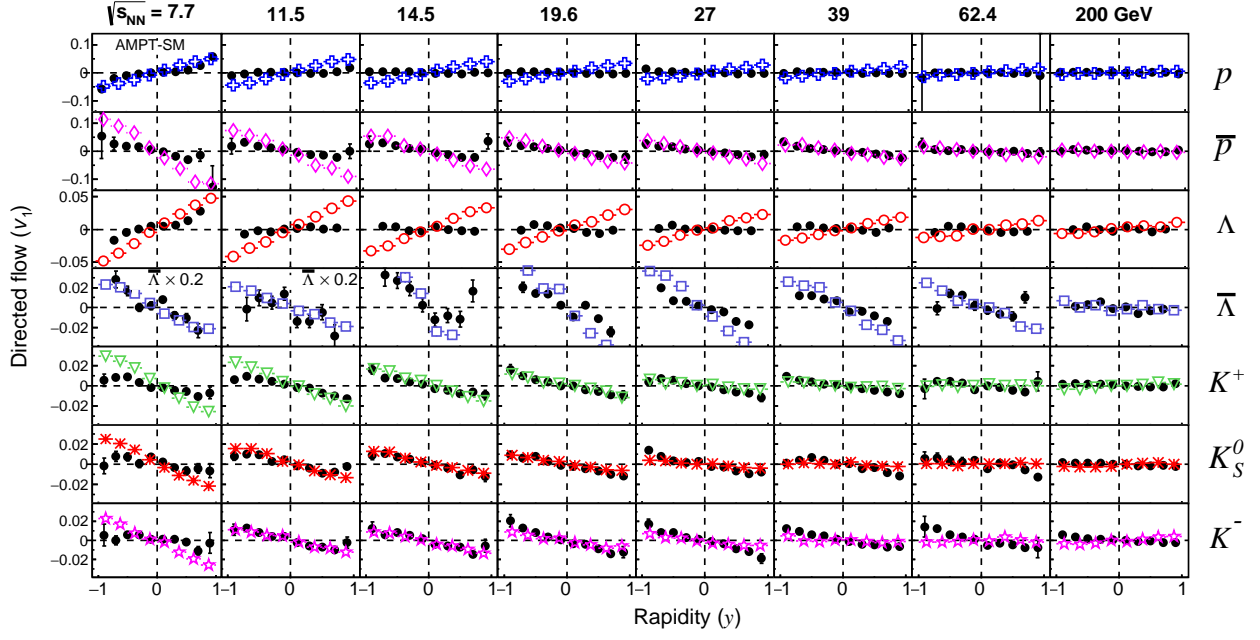


FIG. 3. (Color online) Directed flow (v_1) as a function of rapidity (y) for different identified hadrons (rows) using AMPT-SM model (hadron cascade time, $\tau = 30$ fm/c) is compared with the experimental data (solid circle) from STAR at RHIC [14] in Au+Au collisions at $\sqrt{s_{NN}} = 7.7, 11.5, 14.5, 19.6, 27, 39, 62.4$ and 200 GeV (columns).

cubic function in Au+Au collisions from $\sqrt{s_{NN}} = 7.7$ -200 GeV. The dv_1/dy shows the sign change in between 11.5 to 27 GeV for the fitting range $|y| < 0.6$, which is the same range as the STAR measurement [14]. When the fitting ranges increases, the magnitude of negative slope decreases and for $|y| < 0.6$ the dv_1/dy becomes positive within uncertainty for all measured energies. There is an hint of slope change as observed in STAR [14] although the statistical significance is poor. The slope change of ϕ meson might be due to short range fitting ($|y| < 0.6$) of v_1 as a function of rapidity. There is no difference between the ϕ meson slope calculated using linear and cubic function even though different fitting ranges are considered. One can also observed that there is a sharp increase in the ϕ meson slope with decrease in energy (< 11 GeV) which is similar to the STAR experimental results at RHIC [14].

The energy dependence of proton dv_1/dy receives contribution mainly in two ways (i) v_1 of transported protons from the initial colliding beam rapidity toward the mid-rapidity and (ii) v_1 of protons from pair (particle and anti-particle) production near mid-rapidity. The importance of pair production increases with increase in colliding energy. The "net particle" is a measure of excess particles yield over its anti-particles. It is used to dis-entangle the transported quarks relative to that

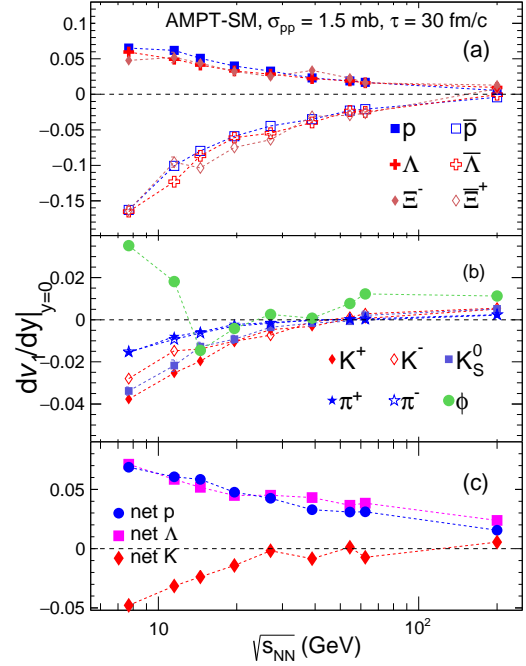


FIG. 4. (Color online) The slope (dv_1/dy) of baryons, mesons and net-p, net- Λ , net- K are shown in upper, middle and lower panels as a function of beam energy for 10-40% centrality, respectively. The dotted lines are smooth curves drawn here to guide the eye.

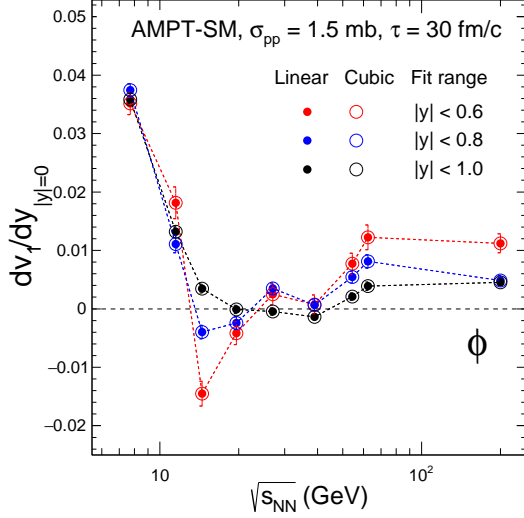


FIG. 5. (Color online) Beam energy dependence of ϕ -meson slope parameter obtained using different fitting ranges and fit functions for 10-40% centrality. The dotted lines are smooth curves drawn here to guide the eye.

of produced in the collisions by using the Eq. 3.

$$[v_1(y)]_p = r(y)[v_1(y)]_{\bar{p}} + [1 - r(y)][v_1(y)]_{\text{net-}p}, \quad (3)$$

where $r(y)$ is the rapidity dependence of anti-proton to proton ratio at each beam energy. The formulae for net-K and net- Λ are defined in the similar way as Eq. 3. Anti-proton v_1 has been proposed as proxy of produced proton v_1 in the Ref [38] and net- p slope is also used to distinguish the transported baryonic matter and hydrodynamic effect [14, 38]. There are also model calculation which suggests that the transported quarks (u and d from initial colliding nuclei) contribute more towards the formation of hadrons like p , Λ and K^+ [32]. Figure 4 (c) shows the net- p , net- Λ and net- K dv_1/dy as a function of beam energy for mid-central (10-40%) Au+Au collisions from $\sqrt{s_{NN}} = 7.7$ -200 GeV. The net- p and net- Λ have positive and similar dv_1/dy unlike the net- K over the measured energy range.

In this analysis, there are several (12) hadrons information which allow us to have a comprehensive study of constituent quark v_1 . The assumption like v_1 is developed in pre-hadronic stage, each quarks have different directed flow and that hadrons are formed via quark coalescence can be tested here. The coalescence sum rule suggests that at smaller azimuthal anisotropy coefficient (v_n), the detected hadron's v_n is sum of their constituent quark's v_n [14]. The popular example of NCQ scaling observed at RHIC and LHC are followed from the

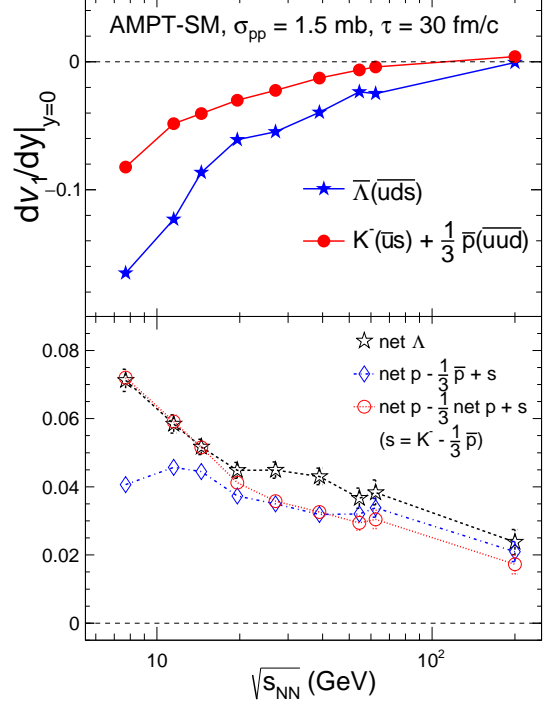


FIG. 6. (Color online) Upper panel shows the comparison of $\bar{\Lambda}(\overline{uds})$ and sum rule test for produced quark ($K^-(\bar{u}s) + \frac{1}{3}\bar{p}(\overline{uud})$) slope as a function of produced beam energy. Lower panel shows another set of sum rule test using net- Λ and net- p for 10-40% centrality in Au+Au collisions using AMPT-SM. The solid and dotted lines are smooth curves drawn here to guide the eye.

coalescence sum rule [15–17].

Figure 6 (upper panel) shows the comparison of $\bar{\Lambda}(\overline{uds})$ and $K^-(\bar{u}s) + \frac{1}{3}\bar{p}(\overline{uud})$ slope as a function of beam energy for 10-40% centrality in Au+Au collisions here from 7.7-200 GeV. The example stated here is the most suitable to test coalescence sum rule because both $\bar{\Lambda}(\overline{uds})$ and $\bar{p}(\overline{uud})$ are produced unlike the u and d quarks which could be either produced or transported. However, by comparing these two cases we have assumed that s and \bar{s} have same flow. The scale factor $\frac{1}{3}$ is due to the assumption that \bar{u} and \bar{d} have the same v_1 . But we found that except for highest energy both of them are found to have different slope, which suggests that these assumptions are not valid for all energies. The dv_1/dy of s and \bar{s} are different except for highest RHIC energy as shown in the Fig 8 for AMPT-SM, $\sigma_{pp} = 1.5$ mb. As per the assumption, one can observe that \bar{u} and \bar{d} have similar slope as shown in the Fig. 8. The STAR measurement at RHIC also found that the slope of $\bar{\Lambda}(\overline{uds})$ and scaled $\bar{p}(\overline{uud})$ have different slope at lower energies [14] and this might be due to the assumption that s and

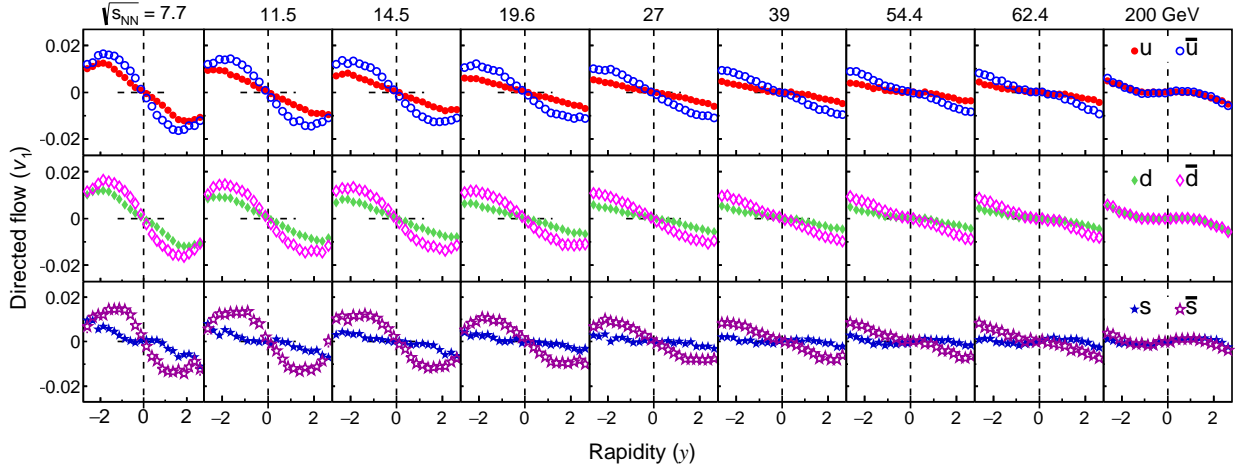


FIG. 7. (Color online) Directed flow (v_1) as a function of rapidity (y) for different quark (anti-quark) solid marker (open marker) are shown in corresponding rows for Au+Au collisions at $\sqrt{s_{NN}} = 7.7, 11.5, 14.5, 19.6, 27, 39, 54.4, 62.4$ and 200 GeV (columns) using AMPT-SM.

\bar{s} have similar v_1 over all measured energy ranges which may not be valid for lower energies.

Figure 6 (lower panel) shows the first case of coalescence sum rule involving u and d quarks which are either transported or produced and hence it is cumbersome to distinguish them in general. However, one can naively expect that at lower beam energy, u and d quarks are mostly transported whereas these quarks are largely produced at high colliding beam energy. In this figure, two different coalescence sum rule scenarios are compared with the net- Λ (open star). First case is the net- p minus u plus s , where u and s quarks are obtained from $\bar{p}/3$ and $K^-(\bar{u}s) - \frac{1}{3}\bar{p}(u\bar{u}d)$, respectively as represented by blue diamond symbol. Here, the produced u quark in net p is replaced by s quark. However, we do not have the corresponding straight forward expression for representing the transported u and d quarks. The sum rule is found to be in a good agreement with net- Λ above 39 GeV and start deviating for lower energies. This observation suggests that the fraction of transported quarks in the constituent quarks assembly of net p increases with decrease in collision beam energy, which imply that the assumption of produced u quark is removed by keeping the term (net $p - \frac{1}{3}\bar{p}$) also starts deviating. The observation of getting the transported quark dominance at lower energy (≤ 39 GeV) in 10-40% centrality Au+Au collisions using AMPT-SM is qualitatively similar to that of observed in STAR experiment at RHIC [14].

The second case of coalescence sum rule i.e. ($\frac{2}{3}\text{net } p + s$) is also shown in the (red open circle

marker) Fig. 6 (lower panel). In this sum rule, it is assumed that in the limit of low beam energy, the constituent quarks of net protons are dominated by transported quarks, and s quark replaced one of the transported quarks. This assumption starts showing disagreement for beam energy greater than 19.6 GeV i.e. the disagreement between black and red markers.

Figure 7 shows the directed flow of partons ($u, \bar{u}, d, \bar{d}, s$ and \bar{s}) systematic evolution in Au+Au collisions from low to high energy ($\sqrt{s_{NN}} = 7.7$ to 200 GeV). All the anti-quarks are produced unlike the quarks which might be either transported or produced depending on the collisions beam energy. So, at highest RHIC energy both the quarks and anti-quarks have same v_1 as these are expected to be mostly produced. However, with decrease in beam energy the v_1 difference between them increases and anti-quarks shows larger directed flow than quarks.

Directed flow slope parameter of quarks, anti-quarks and ϕ meson as a function of beam energy is shown in Fig. 8. The slope of u and d quarks are found to be similar and decreases with increase in beam energy unlike the s quark. All the light anti-quarks (\bar{u}, \bar{d} and \bar{s}) have more steeper negative slope than their corresponding quarks. However, there is a hint of \bar{s} slope deviation from the trend of \bar{u} and \bar{d} with decrease in energy. The ϕ meson slope is scale with its number of constituent quark (2) for better comparison with other partonic slope parameter.

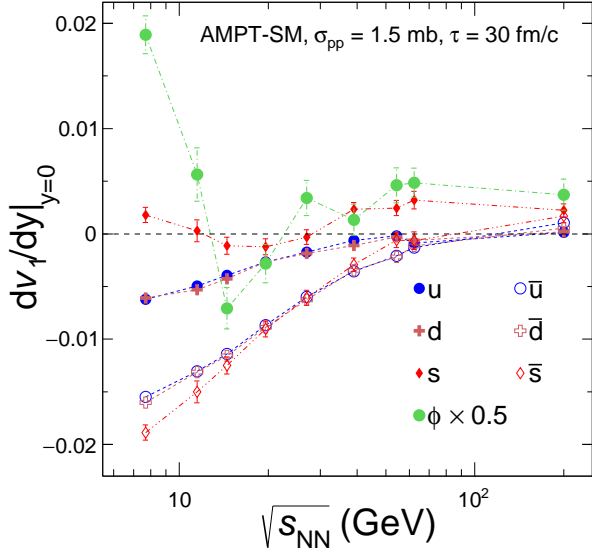


FIG. 8. (Color online) Slope (dv_1/dy) as a function of $\sqrt{s_{NN}}$ for quark, anti-quark and ϕ meson using AMPT-SM for parton-parton cross section (σ_{pp}) of 1.5 mb. The ϕ meson slope is divided with corresponding number of constituent quarks i.e 2.

IV. SUMMARY AND OUTLOOK

A comprehensive study of rapidity-odd component directed flow for charged and identified hadrons in Au+Au collisions (10-40% centrality) for a range of collision beam energies using an improved coalescence AMPT-SM model has been discussed. The coalescence sum rule or commonly known as NCQ scaling is verified using the directed flow measurement of identified hadrons. The analysis performed here are summarized in the following section.

The effect of hadronic interaction on v_1 of charged hadrons and ϕ meson are reported. The v_1 of charged hadrons are found to be not well developed for $\tau = 0.6$ fm/c, because the particles could not get enough time to have interactions unlike the case for $\tau = 30$ fm/c, except for positively charged hadrons at lower energies where the transported quark effect is more dominant. However, the ϕ -meson v_1 is found to be unaffected by hadronic interaction because of its small hadronic cross section and also it decays outside the fireball (life time ~ 42 fm/c). The double sign change of ϕ meson slope in between 11.5 to 27 GeV is observed. This sign change is also found to be an artifact of small fitting ranges while extracting the v_1 slope. The sign change goes away making positive slope

for all measured energies when the linear or cubic function is fitted in a larger rapidity range ($|y| < 1.0$). This observation emphasizes the crucial importance of fitting range while extracting the slope parameter (dv_1/dy) in the real data measurement. Prediction for directed flow as function of rapidity and slope parameter of various identified hadrons in semi-central (10-40%), Au+Au collisions at $\sqrt{s_{NN}} = 54.4$ GeV are reported. The v_1 measurement of Ξ^\pm baryon is predicted for a range of energy and the value is found to be similar to protons and Λ baryons. The v_1 results at higher rapidity range are also shown here, which cover the Event Plane Detector (EPD) pseudo-rapidity (η) range installed in STAR detector at RHIC for BES-II program.

The light quarks such as u and d have similar slope and it decreases with increase in beam energy unlike the s quark. The anti-quarks (\bar{u} , \bar{d} and \bar{s}) have more steeper negative slope than corresponding light quarks and are similar for the measured beam energy range. However, there is a hint that \bar{s} quark slope start deviating from the trend of other light anti-quarks (\bar{u} and \bar{d}) with decrease in energy. The measured baryons (p , Λ and Ξ^-) have similar positive slope and increases with decrease in beam energy unlike their corresponding anti-particles. There is no sign change for p and Λ slope unlike that observed in STAR experiment at RHIC [14]. The slope of π^+ , π^- , K^+ , K^- and K_S^0 mesons are positive at the highest RHIC energy where as it starts decreasing with decrease in beam energy. The slope of K_S^0 is approximately average of K^+ and K^- slope as observed in STAR at RHIC [14].

The test of coalescence sum rule using produced quarks are done by comparing the slope of $\bar{\Lambda}(uds)$ and $K^-(\bar{u}d) + \frac{1}{3}\bar{p}(uud)$. These are found to have different slope and the departure increases with decrease in energy which might be due to break-down of the assumption that s and \bar{s} have same flow over the measured energy range. The slope of net p and net Λ are similar over the measured energy range. The sum rule (net $p - \frac{1}{3}\bar{p} + s$) and net Λ are found to be similar for energy higher than 39 GeV. The deviation at lower energy might be an indication that the assumption of produced u quarks effect can be removed by keeping the term $\frac{2}{3}$. This assumption does not holds reasonable at lower energies which is similar to the observation in STAR at RHIC [14]. The sum rule ($\frac{2}{3}\text{net } p + s$) and net Λ values starts deviating at energy higher than 19 GeV. This sum rule assumes that at lower energy the transported quarks dominates and one of the transported quark of net p is replaced by s quark. Hence, this approximation breaks down in the limit of high beam energy

which is qualitatively similar to the observation in STAR at RHIC [14].

V. ACKNOWLEDGMENTS

This work is supported in part by the MoST of China 973-Project No. 2015CB856901, National Natural Science Foundation of China under Grants No. 11890711 and self-determined research funds of CCNU from the colleges basic research and operation of MOE under Grant No. CCNU18TS031.

-
- [1] H. Sorge, Phys. Rev. Lett. 78, 2309 (1997).
 [2] N. Herrmann, J. P. Wessels, and T. Wienold, Annu. Rev. Nucl. Part. Sci. 49, 581 (1999).
 [3] D. H. Rischke *et al.*, Heavy Ion Phys. 1, 309 (1995).
 [4] H. Stöcker, Nucl. Phys. A 750, 121 (2005).
 [5] Y. Nara *et al.*, Phys. Rev. C 94 034906 (2016).
 [6] S. A. Bass, M. Belkacem and M. Bleicher *et al.*, Progress in Particle and Nuclear Physics, 41, 255-369 (1998).
 [7] M. Bleicher, E. Zabrodin and C. Spieles *et al.*, JPG, 25, 1859-1896 (1999).
 [8] S. Voloshin and Y. Zhang, Z. Phys. C 70665 (1996).
 [9] B. Alver and G. Roland, Phys. Rev. C 81, 054905 (2010), Erratum-ibid.C82:039903 (2010).
 [10] A. M. Poskanzer and S. A. Voloshin, Phys. Rev. C 58, 1671-1678, (1998).
 [11] U. W. Heinz, in Relativistic Heavy Ion Physics, Landolt-Boernstein New Series, Vol. I/23, edited by R. Stock (Springer Verlag, New York, 2010).
 [12] R. Snellings, H. Sorge, S. A. Voloshin, F. Q. Wang and N. Xu, Phys. Rev. Lett. 84, 2803 (2000).
 [13] J. Brachmann *et al.*, Phys. Rev. C 61, 024909 (2000).
 [14] L. Adamczyk *et al.*, (STAR Collaboration) Phys. Rev. Lett. 120, 062301 (2018).
 [15] J. Adams *et al.* (STAR Collaboration), Phys. Rev. Lett. 92, 052302 (2004); J. Adams *et al.* (STAR Collaboration), Phys. Rev. C 72, 014904 (2005); B. Abelev *et al.* (STAR Collaboration), Phys. Rev. C 75, 054906 (2007); B. I. Abelev *et al.* (STAR Collaboration), Phys. Rev. Lett. 99, 112301 (2007).
 [16] S. S. Adler *et al.* (PHENIX Collaboration), Phys. Rev. Lett. 91, 182301 (2003); A. Adare *et al.* (PHENIX Collaboration), Phys. Rev. Lett. 98, 162301 (2007); S. Afanasiev *et al.* (PHENIX Collaboration), Phys. Rev. Lett. 99, 052301 (2007); A. Adare *et al.* (PHENIX Collaboration), Phys. Rev. C 85, 064914 (2012).
 [17] K. Aamodt *et al.* (ALICE Collaboration), Phys. Rev. Lett. 105, 252302 (2010); B. Abelev *et al.* (ALICE Collaboration), JHEP 06, 190 (2015).
 [18] Shusu Shi, Adv. High Energy Phys. 2016, 1987432 (2016).
 [19] J. H. Chena *et al.* Phys. Rev. C 74, 064902 (2006).
 [20] Md. Nasim, Phys. Rev. C 89, 034909 (2014).
 [21] Md. Nasim, B. Mohanty, N. Xu, Phys. Rev. C 87, 014903 (2013).
 [22] L. Adamczyk *et al.*, (STAR Collaboration) Phys. Rev. C 93, 021903 (2016) (R).
 [23] R. J. Fries, B. Müller, C. Nonaka, and S. A. Bass, Phys. Rev. Lett. 90, 202303 (2003).
 [24] R. J. Fries, V. Greco, P. Sorensen, Ann. Rev. Nucl. Part. Sci. 58, 177-205 (2008).
 [25] J. Barrette *et al.*, Phys. Rev. C 50, 1077 (1994).
 [26] S. Albergo *et al.*, Phys. Rev. C 65, 034907 (2002).
 [27] J. Y. Chen, J. X. Zuo, X. Z. Cai, F. Liu, Y.G. Ma and A.H. Tang, Phys. Rev. C 81, 014904 (2010).
 [28] Chong-Qiang Guo, Chun-Jian Zhang and J. Xu, Eur. Phys. J. A 53, 233 (2017).
 [29] Chong-Qiang Guo, He Liu and J. Xu, Phys. Rev. C 98, 024914 (2018).
 [30] Md. Nasim and S. Singha, Phys. Rev. C 97, 064917 (2018).
 [31] S. Singha, P. Shanmuganathan and D. Keane, AHEP 2836989 (2016).
 [32] J. C. Dunlop, M. A. Lisa and P. Sorensen, Phys. Rev. C 84, 044914 (2011).
 [33] Zi-Wei Lin and C. M. Ko, Phys. Rev. C 65, 034904 (2002); Lie-Wen Chen *et al.*, Phys. Lett. B 605 95 (2005); Zi-Wei Lin *et al.*, Phys. Rev. C 72, 064901 (2005).
 [34] X. N. Wang and M. Gyulassy, Phys. Rev. D 44, 3501 (1991).
 [35] B. Zhang, Comput. Phys. Commun. 109, 193 (1998).
 [36] B. A. Li and C. M. Ko, Phys. Rev. C 52, 2037 (1995).
 [37] Y. He, Zi-Wei Lin, Phys. Rev. C 96, 014910 (2017).
 [38] L. Adamczyk *et al.*, (STAR Collaboration) Phys. Rev. Lett. 112, 162301 (2014).
 [39] K. A. Olive *et al.*, (Particle Data Group Collaboration) Chin. Phys. C 38, 090001 (2014).